

SIMPLE RECIPES FOR GROUND SCATTERING IN NEUTRON DETECTOR
CALIBRATION*

T. M. Jenkins
Stanford Linear Accelerator Center
Stanford University, Stanford, California 94305

As potentially hazardous neutron radiation producing devices become more prevalent, there is a corresponding proliferation of monitoring equipment, and a concomitant need to calibrate that equipment. Neutron sources are available for calibration purposes, but elaborate calibration facilities usually are not. Instead, most neutron detector calibration is performed by placing both source and detector at some heights above the ground (or floor), and at a measured distance apart (what we will call a field geometry). Such procedures are also used by larger facilities that do have calibration facilities, but which occasionally need to make calibration checks in the field.

Whenever calibrations are made in this manner, some account must be made for the scattered radiation arriving at the detector. Even though this phenomenon is well-understood (CU54), it is quite often overlooked, probably because of an albedo term which requires looking up albedo data from graphs or tables not always available. While this correction can be quite complex, the geometry portion has been simplified somewhat by Eisenhauer (EI65) who used the con-

(Submitted to Health Physics)

*Work supported by the Department of Energy under contract number DE-AC03-76SF00515.

cepts of specular reflection and virtual images, which are shown in Fig 1. He introduced the term, (r_o/r_i) , where $r_i = r_1 + r_2$ in Fig 1, as useful in the geometry-dependent portion of the scattering problem. In specular reflection, the incident and emerging angles are the same, leading to the following expressions for r_1 and r_2 :

$$r_1 = \left[h_l^2 + \left(\frac{h_l D}{h_l + h_u} \right)^2 \right]^{1/2}, \quad (1)$$

and

$$r_2 = \left[h_u^2 + \left\{ D - \left(\frac{h_l D}{h_l + h_u} \right) \right\}^2 \right]^{1/2}. \quad (2)$$

It makes no difference which is the source and which the detector in Eqn's 1 and 2 above. In the simple case, when $h_l = h_u$, $x = 1/2$, $r_1 = r_2$, and $r_o = D$.

The dose equivalent and fluences arriving at a detector will be given by

$$\text{D.E. (Total)} = \frac{Q C}{4\pi r_o^2} (1 + f(s)) , \quad (3)$$

$$\text{Fluence (Total)} = \frac{Q}{4\pi r_o^2} (1 + f(s)) , \quad (4)$$

where Q is the source strength, f(S) represents the scattered fraction of the direct component which is a function of geometry, that is, of r_i and r_o , and albedo, and C is the source fluence-to-dose equivalent conversion factor. In Eqn. 3, the assumption has been made that C will be the same for both the direct and scattered components, which is clearly not true, but perhaps acceptable for detector calibration purposes.

A few simplifying assumptions can be made for the case of neutron detector calibration in a field geometry. First, from experience one finds that the scattered component arriving at the detector will normally be less than 70% of the direct component. Thus, this scattered component need be determined only to within about 25% for the total dose equivalent or fluence to be known to less than 10% (assuming one knows the direct component to within a percent). Second, within the normal range of source energies, (0.2 to 5 MeV), and for typical source and detector heights (2 to 7 feet) and separation distances (2 to 20 feet), the albedo term is changing only slowly, and will be replaced by a constant. The assumption is made that the scattering material will always be either concrete or earth, and that the albedo is the

same for both. (Simplifying the albedo term to a constant probably won't hold when source and detector are in a vertical line, i.e., when one is above the other.) For the treatment here, we will assume that the dose equivalents or fluences arriving at the detector will be the same for the same values of the ratio of the scattered path, r_1 , to the direct path, r_0 ; that is, $f(S)$ in Eqn's 1 and 2 will be a function of $(r_1 + r_2)/r_0$ only. The actual numerical form of $f(S)$ will then be determined from measurements and from Monte Carlo calculations.

To generate both dose equivalent and fluence data, the Monte Carlo code, MORSE, was run for a PuBe source over a wide range of source and detector heights (source heights from 1 to 5', detector heights from 1 to 20'), and source-detector horizontal separation distances from 2 to 20'. The code was also run for monoenergetic neutrons with energies between 0.16 and 14 MeV, at $h_s = h_d = 5$ feet. The two energies above 4 MeV (10 and 14 MeV) were included to give a better understanding of the energy effects even though they fall outside the intended scope of this study. All sources were isotropic. For fluence responses, an ideal detector with a flat response over the entire spectrum was assumed. The response of the idealized dose equivalent counter was taken from ICRP 21.

To check Eqn's. 3 and 4, the MORSE PuBe data of the total (dose equivalent or fluence) divided by the the direct (dose equivalent or fluence) were plotted versus r_i/r_o in Figs. 2 and 3 for dose equivalent and fluence respectively. As can be seen from these figures, the values for the same r_i/r_o do lie on the same point within a few percent.

The data in Figs 2 and 3 show two slopes, one between values of r_i/r_o of 1.1 and 3, and the other a longer 'tail'. These are probably the scattered component of dose equivalent (or fluence), and the direct component, the latter which would be constant with the value of 1.0. This direct component is subtracted and the resultant plotted as the fraction of the direct component in Fig 4. Before commenting on this figure, the energy dependence of the scattered component should be noted.

Figs. 5 and 6 show the scattered-to-direct results of the different monoenergetic neutron source energies with $h_l = h_u = 5$ feet, again plotted against r_i/r_o . An energy dependence can be seen, particularly in the fluence data. For the dose equivalent data, the spread is random within 25% of some median value, such that a single fit should satisfy the criterion of giving better than 10% overall accuracy. The fluence energy dependence seems to be regular, and may be approximated by a linear fit of the form, $K/(1 + 0.1E)$,

where $K=1.52$ from the figure, and E is in MeV. The scattered fraction, hence, can be fit by the following expressions for the dose equivalent and fluence*:

$$f_d = \frac{0.75 r_i/r_o}{(1 + (r_i/r_o)^3)} \quad , \quad (5)$$

and

$$f_f = \frac{1.52 r_i/r_o}{(1 + 0.1E)(1 + (r_i/r_o)^3)} \quad , \quad (6)$$

where f_d = dose equivalent scattering factor = scattered dose equivalent/direct dose equivalent, and f_f = fluence scattering factor, similarly defined. The fluence data can also be fit (within perhaps 30%) by a single curve about $E = 2.08$ MeV (the median energy of the sources used), simplifying Eqn. 6 to

$$f_f = \frac{1.26 r_i/r_o}{(1 + (r_i/r_o)^3)} \quad (7)$$

Eqn's 5 and 6 are shown in Figs 4, 5 and 6 as solid lines.

Equations 1 and 2 for total dose equivalent and total fluence then become

$$\text{D.E. (Total)} = \frac{Q C}{4\pi r_o^2} \left\{ 1 + \frac{0.75 r_i/r_o}{(1 + (r_i/r_o)^3)} \right\}, \quad (8)$$

$$\text{Fluence (Total)} = \frac{Q}{4\pi r_o^2} \left\{ 1 + \frac{1.52 r_i/r_o}{(1 + 0.1E)(1 + (r_i/r_o)^3)} \right\}, \quad (9)$$

or the simple energy independent form,

$$\text{Fluence (Total)} = \frac{Q}{4\pi r_o^2} \left\{ 1 + \frac{1.26 r_i/r_o}{(1 + (r_i/r_o)^3)} \right\} \quad (10)$$

where C again is the source fluence-to-dose equivalent conversion factor for the source neutrons, and Q, the source strength.

To demonstrate just how well these recipes predict total dose equivalents and fluences for different energy sources, Figs 7 and 8 are included. As can be seen in Fig 7, the MORSE dose equivalent data points are everywhere within 5%

of the calculated curve for all source energies between 0.16 and 14 MeV. The same is true of Fig 8, though there are a family of calculated curves which are energy dependent (only 3 are shown). The data points are everywhere within 5% of the energy dependent curves, and if the 10 and 14 MeV points are excluded, are within 10% of the simple form of the fluence calculation (Eqn 10). Eqn's 8 and 10 are also shown as the solid lines in Figs 2 and 3 for PuBe neutrons.

Measurements of dose equivalent or fluence reported for various combinations of h_l , h_u , and D are rare. The dose equivalent data of Cure (Cu54) do follow the shape of Eqn. 8, but are some 10 - 15% lower, probably due to the use of fluence-to-dose conversion factors no longer valid. The fluence data of DeStaebler (DE65) more-or-less follow the fluence curves, but were affected by the proximity of metal buildings. Measurements made over the years at SLAC with a moderated BF3 at $h_l = h_u = 5$ ft, using PuBe, PuB, PuF and PuLi sources are shown in Fig 9, where the agreement is quite good. Also included in this figure are PuB measurements reported by McCaslin (MC76) where the source and detector were in a vertical line. As expected, these last data do not fit the fluence curves.

The presence of other scattering planes (such as a concrete building) should add to the scattering in the same

way as the ground plane; that is, the fluence or dose equivalent scattering factor, $f(S)$, for each value of r_i/r_0 , will be given by

$$\text{Total } f(S) = N f(S)$$

where N is the number of scattering planes. MORSE does indeed show this to be true.

The report by McCaslin includes measurements made at the low-scattering facility at LLL. The inside dimensions of this concrete room are about 30 feet in width, 40 feet in length and about 24 feet in height, with a metal grill 'working floor' about 9 feet above the concrete floor. While this becomes complicated (there will be rescattering from the walls), still some comparison is possible. For the larger values of r_i/r_0 , N will be 6; that is, all six interior walls contribute at each r_i/r_0 point. For values of r_i/r_0 less than about 3.5, only some of the walls can contribute. This is, of course, due to the actual locations of source and detector which are close to some walls and far from others. For simplicity, N was left at 6 for all values of r_i/r_0 . The data points have been normalized to a value of 1.07 at $r_i/r_0 = 10$ because the original data was normalized to 1 (they assumed no scattering inside the room, and thus normalized their data to 1 at this point). With this renormalization, the agreement is quite good as can be seen in Figure 10.

In summary, Eqn's 8 and 9 or 10 are simple recipes good to within less than 10% over most of the range of usual field calibrations above concrete or earth with normal neutron calibration sources. These recipes do not rely on graphs or albedo information, and are easily solved with a hand-held calculator. As such, it should be relatively simple to account for neutron scattering, whether in the field or in an area where elaborate calibration facilities are not available. However, we must caution the user of these formulae that they are predicated upon idealized fluence and dose equivalent detectors. The standard BF3 detector used at SLAC (6.3 cm polyethylene moderator inside a cadmium sleeve) does follow the fluence curves. The Andersson-Braun rem counter (AN64) also follows the dose curve; other rem responding detectors should do fairly well depending upon how closely they follow the ICRP curve. However, it is always a good idea to check the response of any given detector at least once before relying on a general formulae or sets of curves.

* The author wishes to thank Dr. H. DeStaebler (including help on the form of the fit to Fig 4) and Dr. R.C. McCall for many helpful discussions.

REFERENCES

1. C. Eisenhauer, An Image Source Technique Calculating Reflection of Gamma Rays or Neutrons, H. Phys. 11, 1965.
2. J. W. Cure & G. S. Hurst, Fast-Neutron Scattering: A Correction for Dosimetry, Nucl., 1954.
3. H. DeStaebler, T. Jenkins, PuBe Measurements on the Accelerator Tunnel, SLAC-TN-65-24, 1965.
4. J. B. McCaslin & L. D. Stephens, Effect of Neutron Scattering on the Calibration of Moderated BF₃ Detectors, LBL Health Physics Note #57, 1976.
5. I. O. Andersson, J. Braun, A Neutron Rem Counter, Aktiebolaget Atomenergi Studsvik Rep. AE-132 (1964).

FIGURE CAPTIONS

Figure 1 Geometry used in detector calibration where h_l = height of the lower, h_u = height of the upper and D is the horizontal separation distance.

Figure 2 Ratio of total-to-direct dose equivalents from MORSE for PuBe neutrons plotted versus r_i/r_o . The following symbols are given as source height/detector height (in cm). \times = 152.5/152.5, \circ = 91.5/152.5, 152.5/91.5, \blacktriangle = 61.5/152.5, 152.5/61.5, \blacksquare = 30.5/152.5, \blacktriangledown = 152.5/244, \blacklozenge = 152.5/305, \bullet = 152.5/610, 91.5/91.5, \bullet = 152.5/30.5.

Figure 3 Ratio of total-to-direct fluence from MORSE for PuBe neutrons plotted versus r_i/r_o . The following symbols are given as source height/detector height (in cm) \times = 152.5/152.5, \circ = 91.5/152.5, 152.5/91.5, \blacktriangle = 61.5/152.5, \blacksquare = 30.5/152.5, \blacktriangledown = 152.5/244, \blacklozenge = 152.5/305, \bullet = 152.5/610, 91.5/91.5, 152.5/61, \bullet = 152.5/30.5.

Figure 4 Scattered dose equivalents and fluences from MORSE for PuBe neutrons versus r_i/r_o . Solid lines = Eqn's 5, and 6 with $E = 4.2$ MeV.

Figure 5 Ratio of scattered-to-direct dose equivalents from MORSE at $h_l = h_u = 152.5$ cm for monoenergetic sources versus r_i/r_o . $\dagger = 14$ MeV, $\circ = 10$ MeV, $\Delta = 4$ MeV, $\nabla = 2.3$ MeV, $\square = 1.1$ MeV, $\times = 0.5$ MeV, $\diamond = 0.16$ MeV, Solid line = Eqn. 5.

Figure 6 -Ratio of scattered-to-direct fluences from MORSE at $h_l = h_u = 152.5$ cm versus r_i/r_o . $\dagger = 14$ MeV, $\circ = 10$ MeV, $\Delta = 4$ MeV, $\nabla = 2.3$ MeV, $\square = 1.1$ MeV, $\times = 0.5$ MeV, $\diamond = 0.16$ MeV, Solid lines = Eqn. 6 with $E = 1, 2, 4.2$ and 10 MeV.

Figure 7 Ratio of total-to-direct dose equivalents from MORSE at $h_l = h_u = 152.5$ cm versus r_i/r_o . $\times = 14$ MeV, $\circ = 10$ MeV, $\square = 4$ MeV, $\Delta = 2.3$ MeV, $\nabla = 1.1$ MeV and PuBe, $\bullet = 0.5$ MeV, $\diamond = 0.16$ MeV, Solid line = Eqn. 8.

Figure 8 Ratio of total-to-direct fluences from MORSE versus r_i/r_o . $\times = 14$ MeV, $\circ = 10$ MeV, $\square = 4$ MeV, $\Delta = 2.3$ MeV, $\nabla = 1.1$ MeV, $\diamond =$ PuBe, $\bullet = 0.5$ and 0.16 MeV, Solid lines = Eqn. 9 with $E = 1, 3$ and 10 MeV.

Figure 9 Ratio of total-to-direct fluences measured with a moderated BF3 detector for PuBe neutrons at $h_l = h_u = 5$ feet, versus r_i/r_o . $\circ =$ PuBe, $\Delta =$ PuBe, PuB, PuF, $\times =$ PuLi, $\bullet =$ PuB source and detector in vertical plane (MC 76). Solid line = Eqn. 10.

Figure 10 Comparison between calculations with $N=6$ and measurements inside the LLL calibration room with a PuBe source.

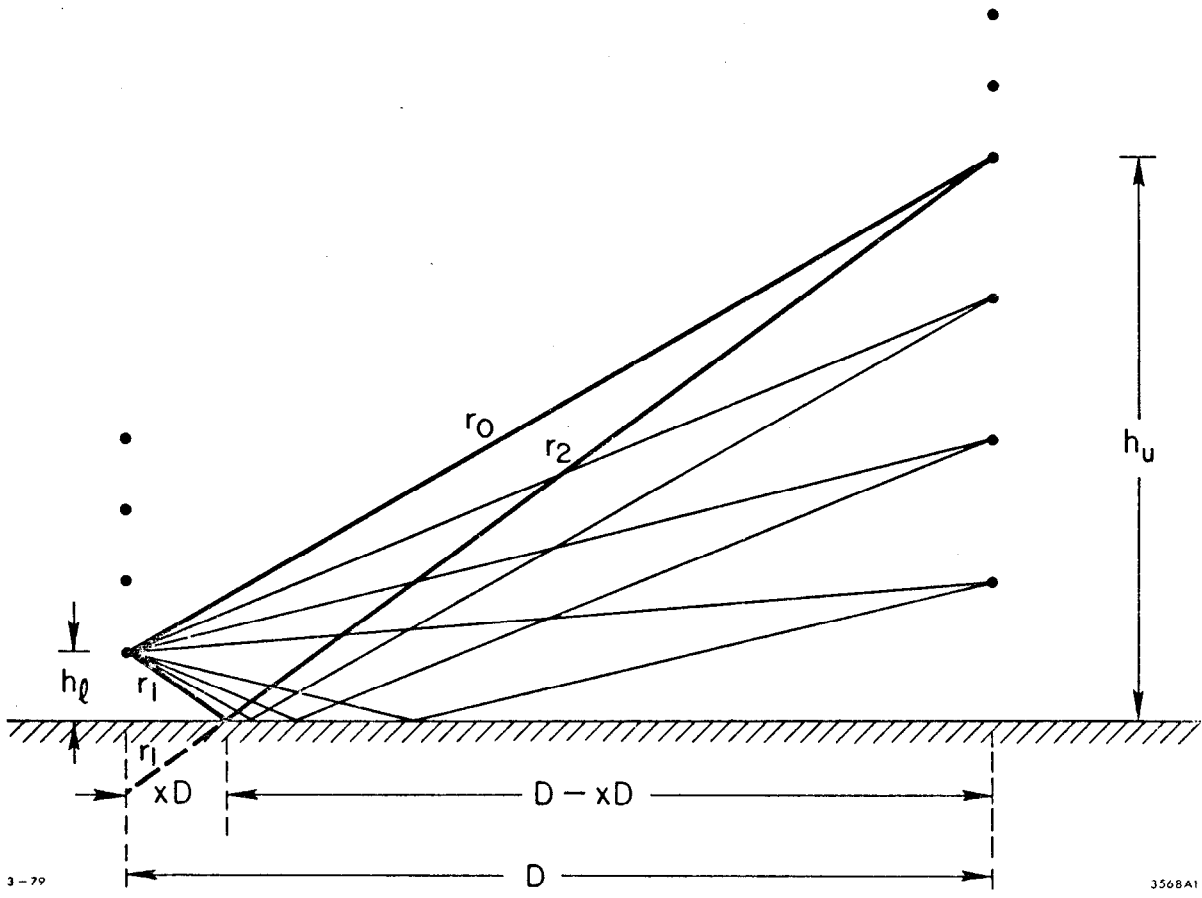
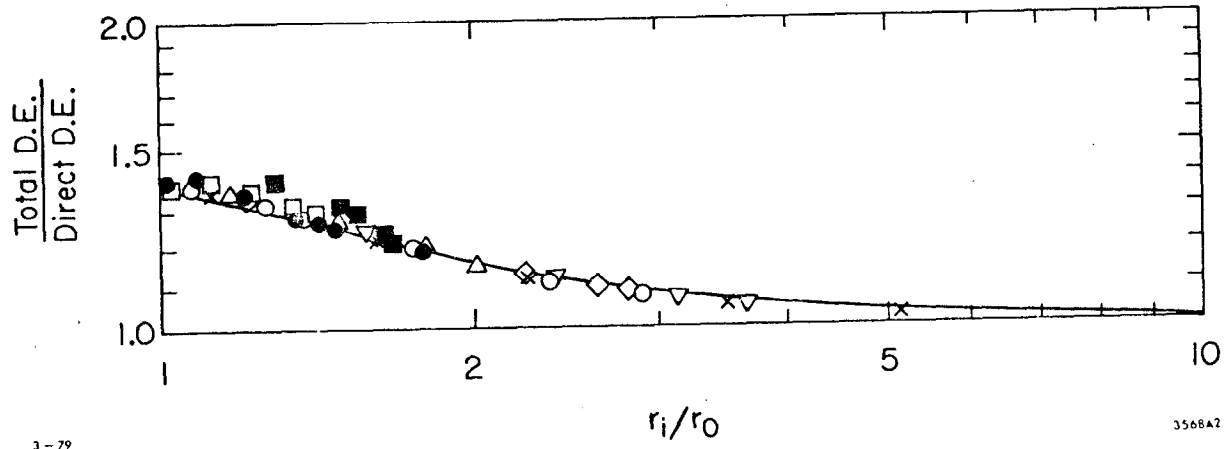


Fig. 1



3-79

3568A2

Fig. 2

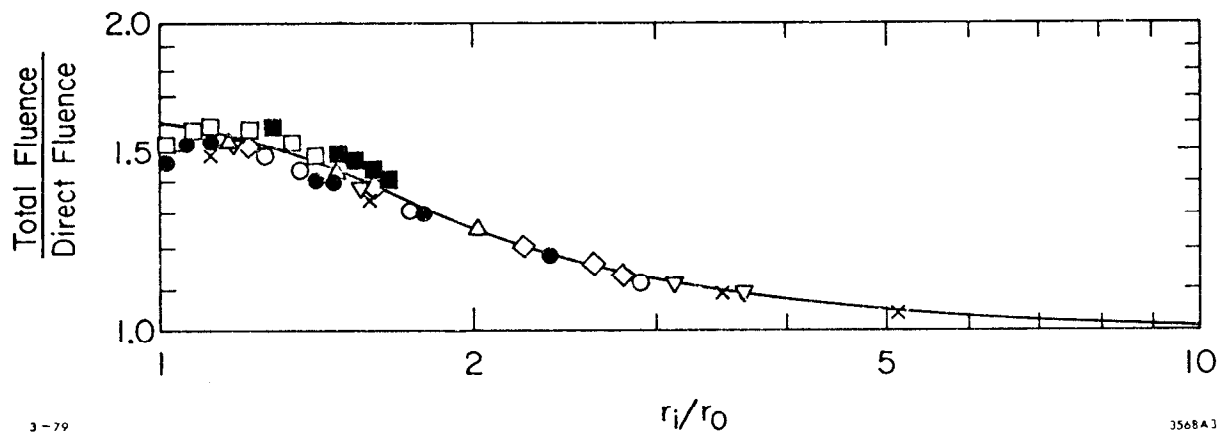


Fig. 3

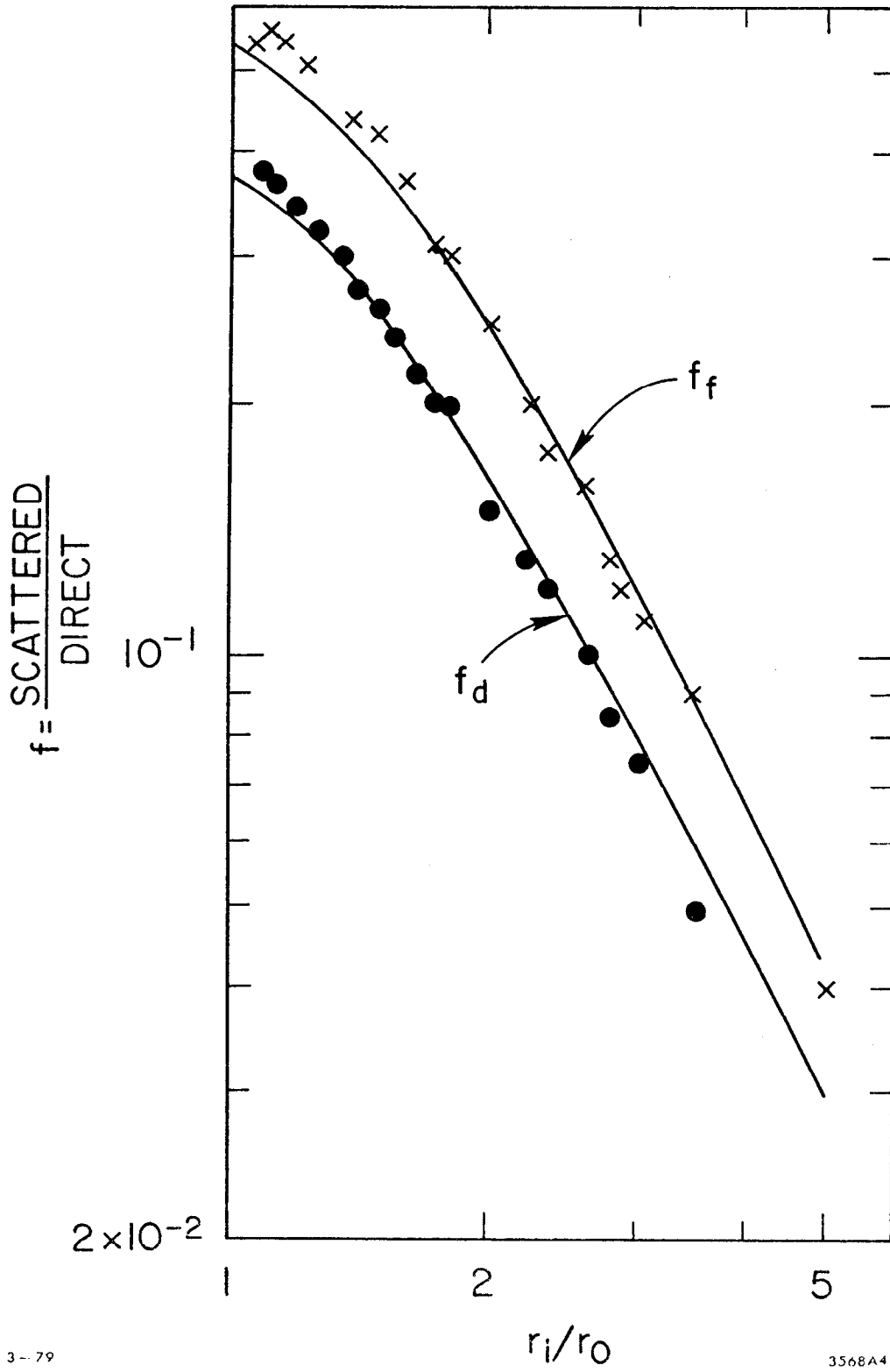


Fig. 4

$$f_d = \frac{\text{SCATTERED D.E.}}{\text{DIRECT D.E.}}$$

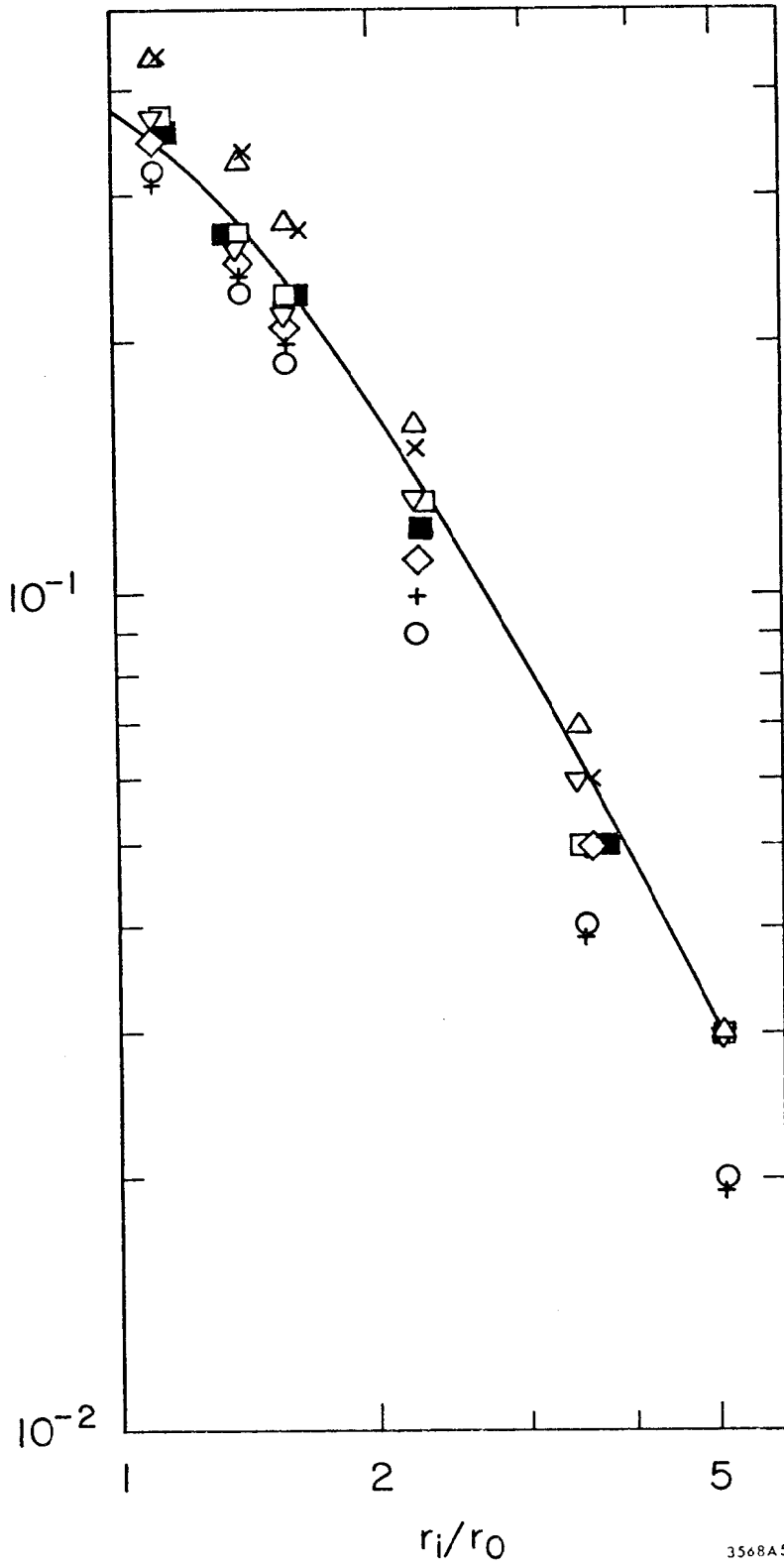


Fig. 5

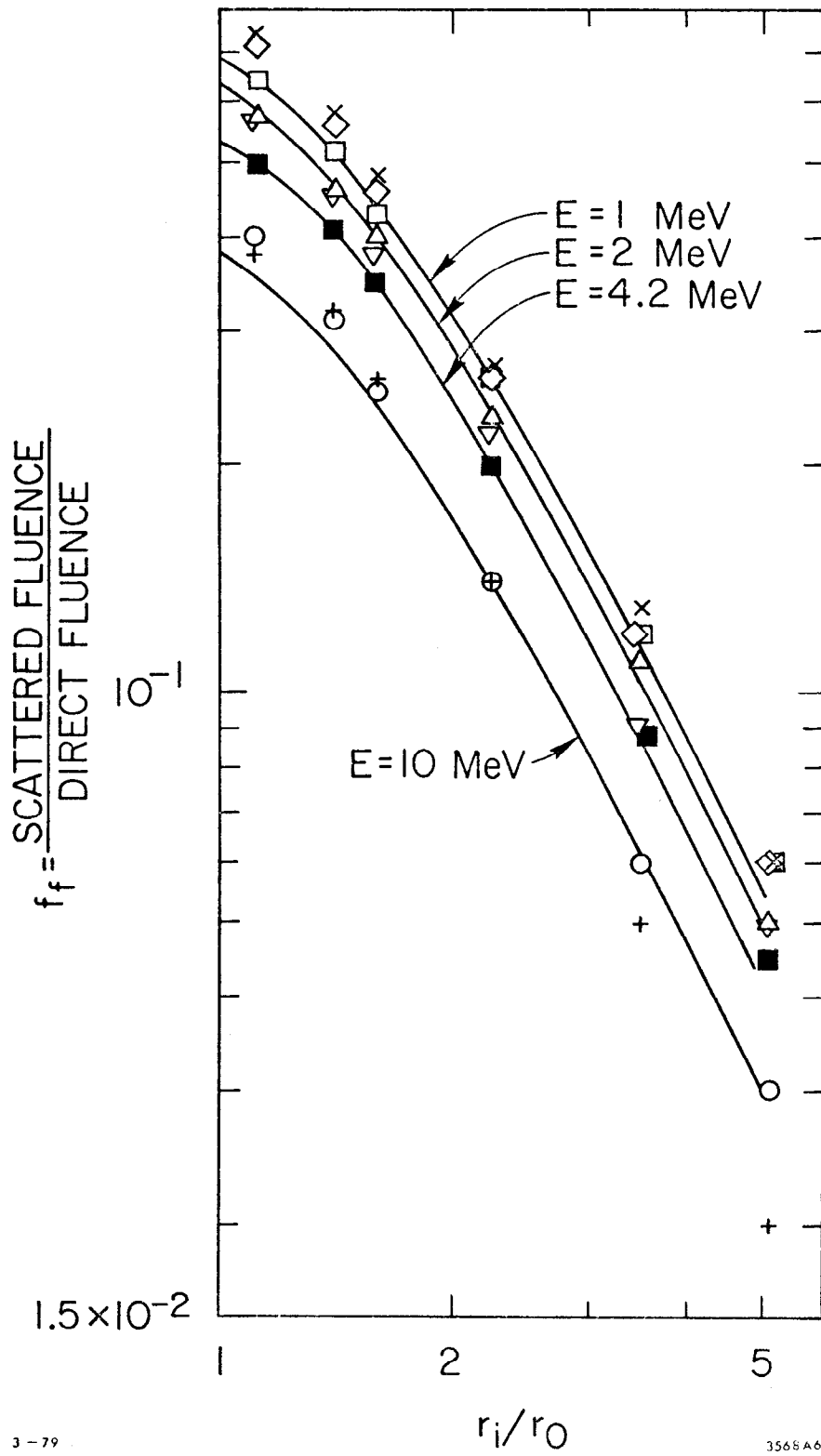


Fig. 6

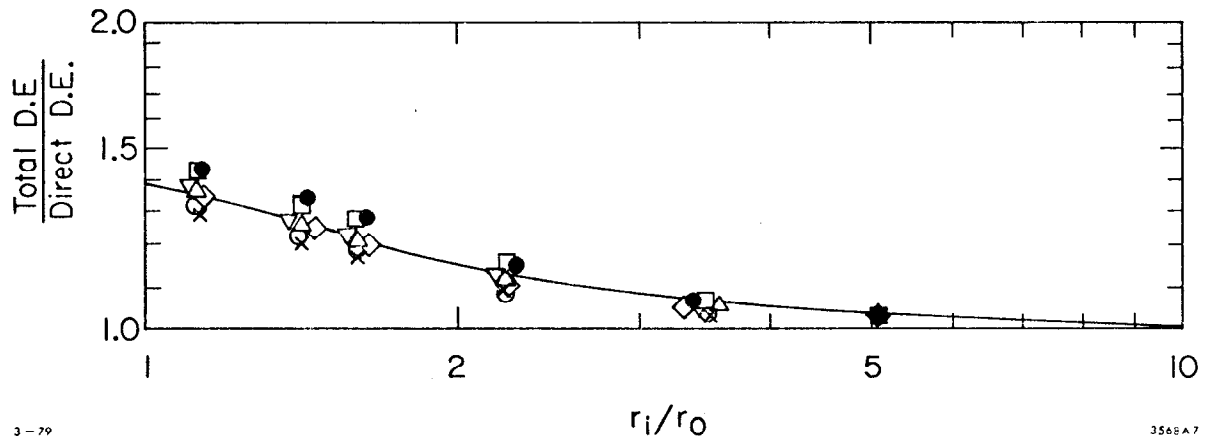


Fig. 7

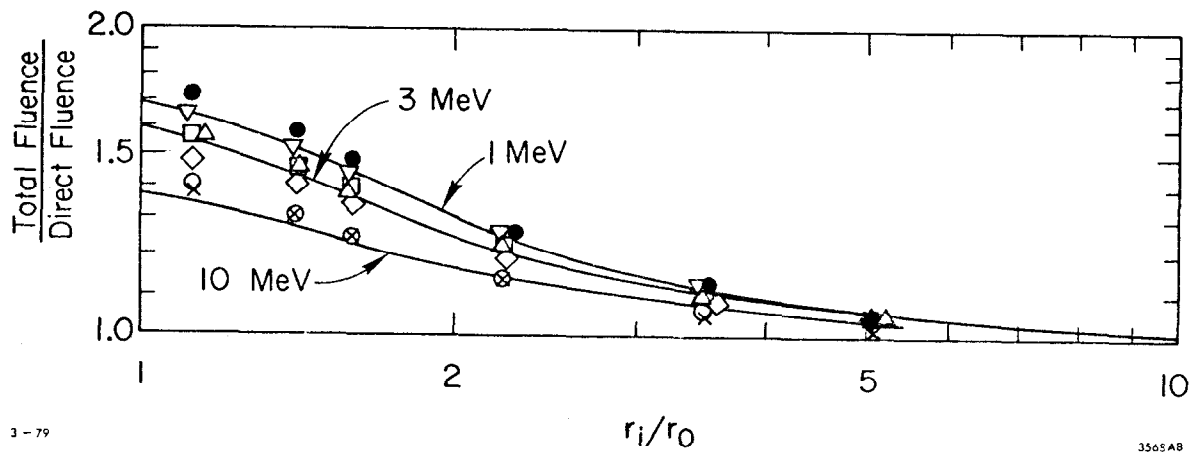


Fig. 8

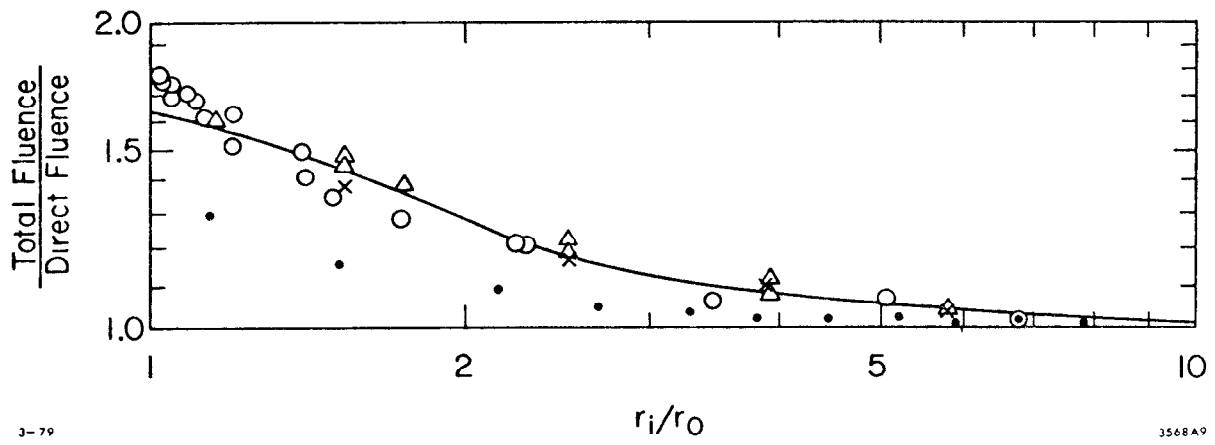


Fig. 9

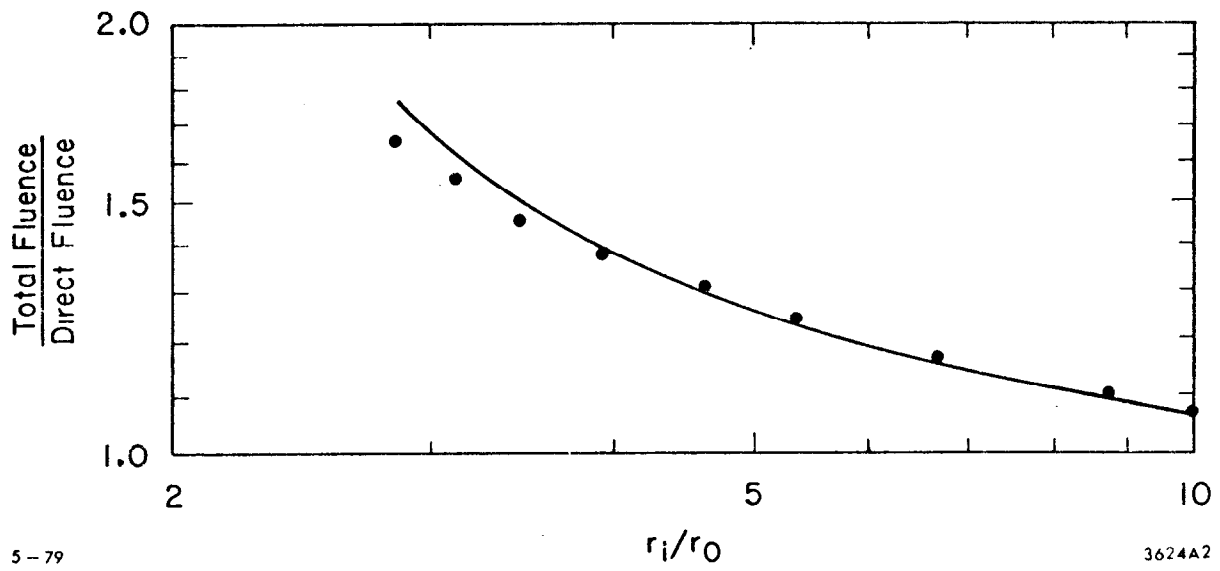


Fig. 10